Gemini Surfactants with a Disaccharide Spacer

Fredric M. Menger* and Bessie N. A. Mbadugha

Contribution from the Department of Chemistry, Emory University, Atlanta, Georgia 30322

Received September 8, 2000

Abstract: A gemini surfactant is an amphiphile possessing (in sequence) the following: hydrocarbon tail/polar group/spacer/polar group/hydrocarbon tail. Widespread interest in geminis has emerged recently from both industrial and academic laboratories. In the present contribution, two related families of geminis have been synthesized, both with trehalose, a disaccharide, as a polar spacer. One family, Series-A, is nonionic and has amide groups separating the long chains from the trehalose spacer. The other family, Series-B, has quaternary ammonium ions connecting the long chains to the trehalose spacer. It was found that Series-A geminis are water insoluble despite the two amides and multiple hydroxyls. When hydrated or extruded, these geminis form microscopically visible vesicular and tubular structures above their transition temperatures (which were determined calorimetrically). Insoluble monomolecular films, constructed from these geminis, have interfacial areas that are dominated by the sugar spacer although intermolecular chain/chain interactions seem to stabilize the films. Thus, the behavior of Series-A geminis in many ways parallels that of phospholipids and simple double-chain surfactants. It is as if the trehalose is less of a spacer than a large but conventional headgroup. In contrast, cationic Series-B geminis are water soluble and form micelles with critical micelle concentrations an order of magnitude lower than that of corresponding conventional surfactants. Molecular modeling using the Amber* force field explains the difference in properties between the two families of geminis. Series-A are tubular in shape and thus prefer bilayer packing as do other amphiphiles in which the headgroups are similar in width to the sum of the tail diameters. Series-B geminis are conical-shaped and pack more readily into spherical micelles. This work entails synthesis, tensiometry, conductance, microscopy, surface balance studies, calorimetry, light scattering, and molecular modeling. In colloid chemistry, a balanced perspective cannot be achieved by one methodology alone but only through the pursuit of consilience among multiple approaches.

Introduction

It is worth inquiring why certain areas of chemistry, such as gemini surfactants, seemingly acquire a sudden and irresistible allure.[1] The fact remains that the most fundamental and lasting objective of organic chemistry is not the production of new compounds per se, but rather the production of interesting and useful properties. Since gemini surfactants have been shown to possess a variety of unique properties,[1] the compounds have attracted worldwide scrutiny. Thus, geminis are finding their way into skin care formulations,[2] antibacterial regimens,[3] the preparation of high-porosity materials,[4] analytical separations,[5] solubilization processes,[6] and antipollution protocols.[7] Nearly 100 patents dealing with geminis are now in force.

The development of gemini chemistry has not simply been an accumulation of data on a new family of surfactants. It has been a change of landscape; a change in the way colloid chemists think. Freed from the limitations of mundane conventional surfactants, it is now possible, with the aid of organic synthesis, to roam freely among a colorful array of virgin amphiphiles.

What exactly is this gemini surfactant of which we write? Instead of having a single hydrocarbon tail connected to an ionic or polar headgroup (as in a conventional surfactant), geminis have the arrangement shown below.

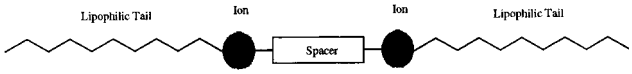

The two terminal hydrocarbon tails can be short or long; the two polar headgroups can be cationic, anionic, or nonionic; the spacer can be short or long, flexible or rigid, polar or nonpolar (see Scheme 1 in ref 1).[8−12] The geminis need not be symmetrically disposed about the center of the spacer.[13,14] Clearly, a wealth of compounds lies within the compass of synthetic possibilities.

This paper deals with geminis having trehalose as the spacer (Scheme 1). Series-A consists of trehalose having the 6- and

(1) Menger, F. M.; Keiper, J. S. *Angew. Chem., Int. Ed.* **2000**, *39*, 1906−1920.
(2) Kwetkat, K. (Huls A.-G.). WO 9731890, 1997; *Chem Abstr*. **1997**, *127*, 249754r.
(3) Pavlíková, M.; Lacko, I.; Devínský, F.; Mlynarcík, D. *Collect. Czech. Chem. Commun*. **1995**, *60*, 1213−1228.
(4) Van Der Voort, P.; Mathieu, M.; Mees, F.; Vansant, E. F. *J. Phys. Chem. B* **1998**, *102*, 8847−8851.
(5) Chen, K.; Locke, D. C.; Maldacker, T.; Lin, J.-L.; Aawasiripong, S.; Schurrath, U. *J. Chromatogr. A* **1998**, *822*, 281−290.
(6) Dreja, M.; Tieke, B. *Langmuir* **1998**, *14*, 800−807.
(7) Li, F.; Rosen, M. J. *J. Colloid Interface Sci*. **2000**, *224*, 265−271.
(8) (a) Diamant, H.; Andelman, D. *Langmuir* **1994**, *10*, 2910−2916. (b) Diamant, H.; Andelman, D. *Langmuir* **1995**, *11*, 3605−3606.
(9) Hirata, H.; Hattori, N.; Ishida, M.; Okabayashi, H.; Frusaka, M.; Zana, R. *J. Phys. Chem*. **1995**, *99*, 17778−17784.
(10) (a) De, S.; Aswal, V. K.; Goyal, P. S.; Bhattacharya, S. *J. Phys. Chem*. **1996**, *100*, 11664−11671. (b) Aswal, V. K.; De, S.; Goyal, P. S.; Bhattacharya, S.; Heenan, R. K. *Phys. Rev. E* **1998**, *57*, 776−783.
(11) (a) Maiti, P. K.; Chowdhury, D. *Europhys. Lett*. **1998**, *41*, 183−188. (b) Maiti, P. K.; Chowdhury, D. *J. Chem. Phys*. **1998**, *109*, 5126−5133.
(12) Menger, F. M.; Keiper, J. S.; Azov, V. *Langmuir* **2000**, *16*, 2062−2067.
(13) Peresypkin, A. V.; Menger, F. M. *Org. Lett*. **1999**, *1*, 1347−1350.
(14) Renouf, P.; Mioskowski, C.; Lebeau, L.; Hebrault, D.; Desmurs, J.-R. *Tetrahedron Lett*. **1998**, *39*, 1357−1360.

10.1021/ja0033178 CCC: $20.00
Published on Web 01/16/2001

Scheme 1

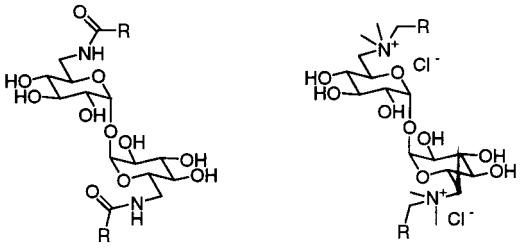

A-8. R = C_7H_{15}
A-10. R = C_9H_{19}
A-12. R = $C_{11}H_{23}$
A-14. R = $C_{13}H_{27}$
A-16. R = $C_{15}H_{31}$
A-18. R = $C_{17}H_{35}$
A-18U. R = $C_{17}H_{33}$ (*cis*-9)

B-12. R = $C_{11}H_{23}$
B-14. R = $C_{13}H_{27}$

6′-hydroxyls replaced by long-chained amides. Series-B has long-chained quaternary ammonium groups at the 6- and 6′-positions. Our selecting trehalose as the sugar-spacer was not arbitrary. First, trehalose is a disaccharide which allowed separation of the two hydrocarbon chains by a considerable distance. Restricted intramolecular chain/chain interactions in geminis is a structural feature that has been only briefly examined in the past.[15] Second, trehalose (a sugar isolated from a variety of natural sources including bacteria, algae, insects, and plants) serves to protect biological membranes from the stress of dehydration.[16] Our trehalose geminis were therefore of interest to us in connection with "cytomimetic" modeling of biological membranes.[17] Third, trehalose was attractive from a pragmatic standpoint because it comprises two identical D-glucopyranose units. This simplified the synthesis and analysis of the compounds by halving the number of chemically distinct hydroxyls relative to most other disaccharides. But symmetry notwithstanding, the synthetic pathways to pure trehalose geminis (Schemes 2 and 3) were admittedly a tedious preamble to the physical chemistry that followed.

Sugar surfactants are well-known, and a literature review here must necessarily lace brevity with vagueness. We confront the issue, after a fashion, by means of Scheme 4. Illustrated therein is a variety of sugar surfactants, including a gemini, that have been synthesized in the past.[18−26] Reference citations within the corresponding papers blanket the subject reasonably well. To our knowledge, the structures under consideration in the present manuscript are new and unexplored with one exception: A 1986 Japanese patent found certain Series-A compounds, made apparently by a different route, to be active against Ehrlich carcinoma in mice.[27]

Results and Discussion

The means by which we acquired Series-A and -B trehalose geminis is recounted in Schemes 2 and 3 as well as in the Experimental Section. A few additional comments serve to embellish this information. The most obvious a priori route to Series-B-type trehalose geminis would be direct displacement of the tosylate groups of **2** by a long-chained tertiary amine. Despite repeated attempts along these lines, only decomposition products or starting materials were obtained. As indicated by Scheme 2, however, we did manage to substitute the two tosylates of **2** with azides to give **3**. A literature procedure was adopted here[28] except for the fact that, owing to safety considerations, HMPA was replaced by DMPU as the solvent. Bis-azide **3** was then subjected to the Staudinger reaction[25,29] to give, in a single step, the long-chain bis-amides **4a**−**g** which, in turn, had only to be deprotected to obtain the Series-A geminis. In Scheme 3, azide reduction of the deprotected sugar **5** converted the compound into the bis-primary amine dihydrochloride **6**. Reductive amination of long-chain aldehydes with **6** and pyridine−borane complex[30] gave trehalose derivatives **7**. Only poor yields for this reaction were achieved using $NaBH_3CN$ as the reducing agent. After methylation of **7** with methyl iodide, followed by ion exchange (to facilitate purification and to promote solubility), we arrived at the Series-B trehalose geminis.

One must always be alert for the presence of impurities and the substantial effect they can have on surfactant properties. (It might be said that impure thoughts are ever-present among colloid chemists.) In our case, precursors **4a**−**g** in Scheme 2 were purified by column chromatography prior to deprotection to the final Series-A geminis. The latter were characterized by ^1H and ^{13}C NMR, high-resolution FAB MS, and elemental analysis. In most cases, the experimental percentages of C, H, and N agreed with theory to better than 0.30% absolute. Similar good agreement in C, H, N, and Cl elemental analyses were found for the two Series-B geminis. Surface tension data never showed the peculiar "dip" indicative of impurities.

Series-A Trehalose Geminis

Our first twinkle of surprise came with the discovery that Series-A trehalose geminis are water insoluble. For example, **A-12**, **A-14**, and **A-16** (the numbers referring to the chain-lengths) leave a precipitate when 2 mg are vortexed in 1 mL of warm water. **A-10** forms a cloudy suspension upon such treatment even at 70 °C. **A-8** is soluble up to only 1−2 mM at room temperature (a concentration at which, according to dynamic light scattering, micelle-sized aggregates are formed). Naively, one might have expected a far greater solubility for **A-8** because the molecule comprises six hydroxyls and two amides. Although related 6-amido-6-deoxyhexose derivatives

(15) Menger, F. M.; Littau, C. A. *J. Am. Chem. Soc*. **1993**, *115*, 10083−10090.
(16) (a) Hanamura, T.; Asakawa, N.; Inoue, Y.; Sakurai, M. *Chem. Lett.* **1998**, 713−714. (b) Engelsen, S. B.; Pérez, S. *J. Phys. Chem. B* **2000**, *104*, 9301−9311.
(17) Menger, F. M.; Angelova, M. I. *Acc. Chem. Res*. **1998**, *31*, 789−797.
(18) Schmidt, R. R.; Jankowski, K. *Liebigs Ann*. **1996**, 867−879.
(19) Dahloff, W. V. *Liebigs Ann. Chem*. **1990**, 1025−1027.
(20) Lubineau, A.; Augé, J.; Drouillat, B. *Carbohydr. Res*. **1995**, *266*, 211−219.
(21) Miethchen, R.; Holz, J.; Prade, H.; Liptak, A. *Tetrahedron* **1992**, *48*, 3061−3068.
(22) Pestman, J. M.; Terpstra, K. R.; Stuart, M. C. A.; van Doren, H. A.; Brisson, A.; Kellogg, R. M.; Engberts, J. B. F. N. *Langmuir* **1997**, *13*, 6857−6860.
(23) Polidori, A.; Pucci, B.; Riess, J. G.; Zarif, L.; Pavia, A. A. *Tetrahedron Lett*. **1994**, *35*, 2899−2902. (b) Polidori, A.; Braun, O.; Mora, N.; Pucci, B. *Tetrahedron Lett*. **1997**, *38*, 2475−2478.
(24) André-Barrès, C.; Madelaine-Dupuich, C.; Rico-Lattes, I. *New J. Chem*. **1995**, *19*, 345−347.
(25) Maunier, V.; Boullanger, P.; Lafont, D.; Chevalier, Y. *Carbohydr. Res*. **1997**, *299*, 49−57.
(26) van Doren, H. A.; Smits, E.; Pestman, J. M.; Engberts, J. B. F. N.; Kellogg, R. M. *Chem. Soc. Rev*. **2000**, *29*, 183−199.
(27) Shibata, A.; Kamiyama, H.; Kuraishi, T.; Kukita, K.; Katori, T. (S. S. Pharmaceutical Co., Ltd.) JP 84253634 841130, 1984.
(28) Birch, G.; Richardson, A. C. *Carbohydr. Res*. **1968**, *8*, 411−415.
(29) Saxon, E.; Armstrong, J. I.; Bertozzi, C. R. *Org. Lett*. **2000**, *2*, 2141−2143.
(30) Bomann, M. D.; Guch, I. C.; DiMare, M. *J. Org. Chem*. **1995**, *60*, 5995−5996.

Scheme 2

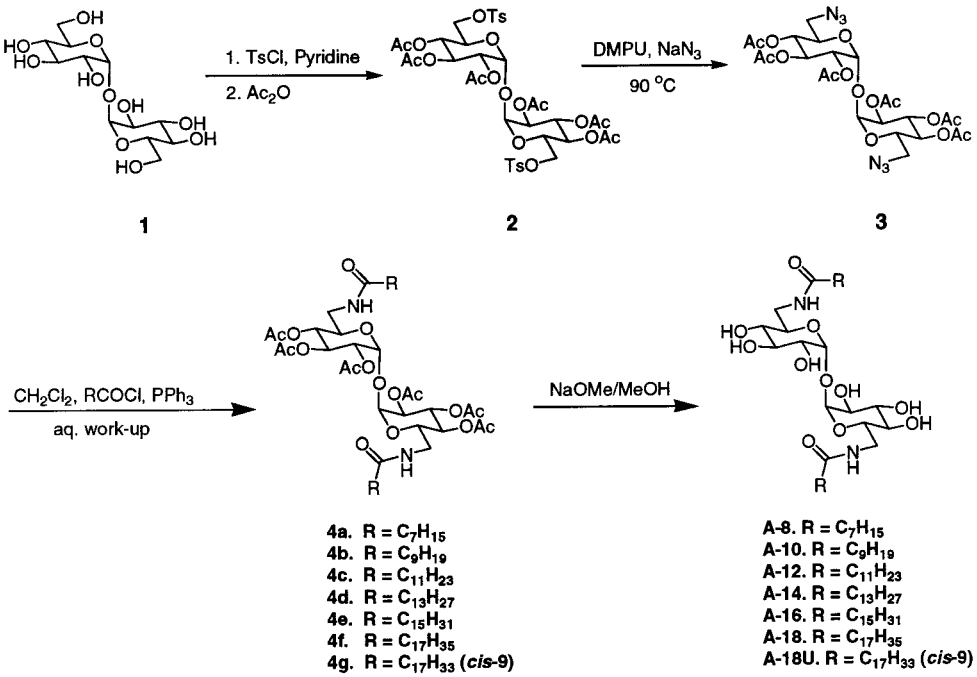

Scheme 3

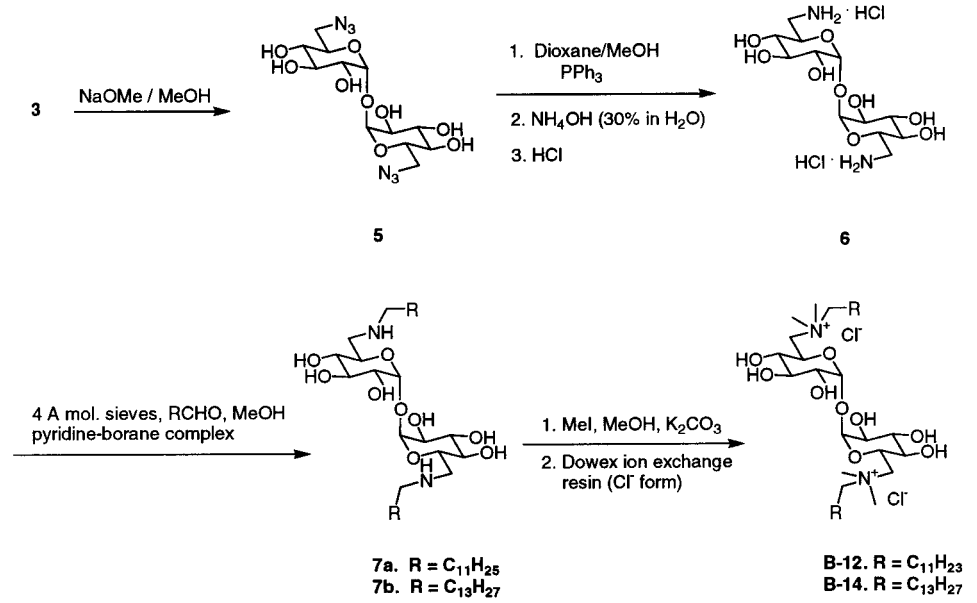

require heating to dissolve them,[25] many alkylated monosaccharides (e.g., octyl glucoside and methyl 6-*O*-(*N*-heptylcarbomoyl)-α-D-glucopyranoside or "Hecameg" drawn below)

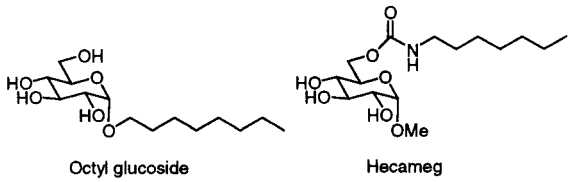

are water soluble. Yet **A-8** is not similarly endowed. The lesson here is that, to use a cliché, our gemini is more (or less) than the sum of its parts. Cliché or not, the unique properties of geminis are dependent upon it.

Solubility is a mundane and often ignored parameter, difficult to measure, and even more difficult to understand. A solid might be insoluble in water owing to strong crystal forces, the nature of which is frequently obscure even with the availability of X-ray data. In our case, intra-[25] and intermolecular hydrogen-bonding involving the amide may contribute to the thermodynamic stability of the solid state. Insolubility can also stem from unfavorable solvation and aggregation effects in solution. Series-A trehalose geminis might resist dissolution because they are unable to form hydrophilic micellar aggregates in a manner possible with corresponding single-chained segments. This speculation becomes credible when it is considered that the two chains of the geminis are situated on the far ends of a disaccharide where intramolecular chain/chain interactions are partially impaired. The subject of chain association will be addressed later.

Water insolubility of the Series-A trehalose geminis allows us to propound their behavior as monomolecular films resting

Scheme 4

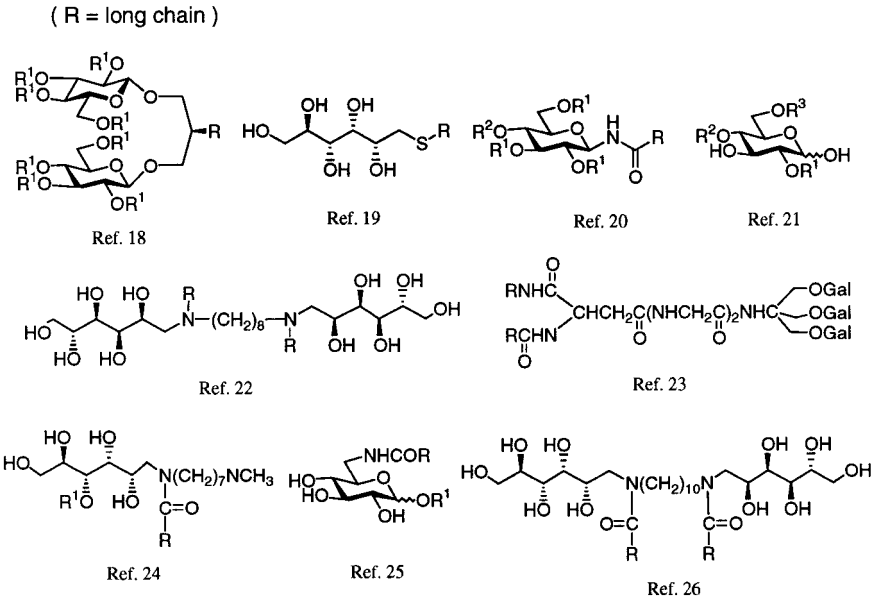

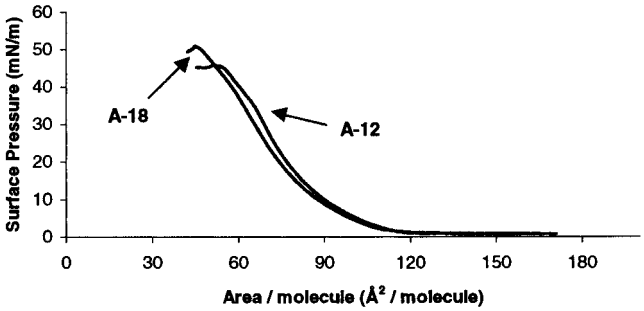

Figure 1. Pressure−area isotherms of **A-12** and **A-18** obtained with a surface balance, showing lift-off areas of approximately 120 Å^2 at 23 °C. Plots are averages of 10 scans taken for each surfactant.

upon a water subphase.[31−33] With the aid of a surface balance, gemini monolayers were slowly compressed by a moveable barrier during which the film pressure and area were monitored. The resulting "pressure−area isotherms" reveal the packing behavior of the gemini molecules within the monolayers. Representative isotherms are given for **A-12** and **A-18** in Figure 1 where the ordinate is the surface pressure applied to the monolayer (in mN/m or, identically, in dynes/cm), while the abscissa is the area per molecule (in Å^2) occupied in the film at a given pressure.

Figure 1 shows lift-off areas (i.e., areas at which the isotherms depart from the baseline owing to intermolecular contacts) for **A-12** and **A-18** (and intermediate chain lengths not plotted here) of about 120 Å^2. By way of calibration, an alkyl glucoside occupies an average area of 49 Å^2,[34,35] whereas the molecular cross-section of a hydrocarbon chain is about 20 Å^2.[33] The simplest explanation for Figure l, buttressed by the near identical isotherms of **A-12** and **A-18**, is that the trehalose spacer, rather than its hydrocarbon substituents, dominates the interfacial packing. Apparently, the alkyl groups project from the air/water interface into the air and contribute little to the geometric requirements of the film. Nonetheless, intermolecular van der Waals forces among the chains stabilize the film. This follows from the fact that the collapse pressure (i.e., the high pressure at which the monomolecular films ultimately "break") correlates positively with chain length as seen, for example, with **A-18** (53 mN/m) and **A-12** (47 mN/m).

When solid **A-10** and **A-12** geminis were immersed in water and examined by optical microscopy 3−4 h later, vesicular structures had emanated from the surfaces (Figure 2). And when milky suspensions of 1 mM **A-10** were extruded multiple times through a 100 nm polycarbonate filter, there was formed, according to dynamic light scattering, a population of 100 nm diameter vesicles. Hydration of solid **A-l4**, **A-16**, and **A-18**, on the other hand, produced no vesicles at room temperature. The difference in behavior between **A-10**/**A-12** and their higher homologues suggested that phase states were playing a role here. Thus, shorter-chained lipids are known to exist in the fluid "liquid crystalline" phase at room temperature, while longer-chained lipids prefer the highly ordered "gel" phase.[36] A gel-to-liquid-crystalline conversion occurs at a transition temperature T_m. Above the T_m, water can be admitted among the bilayers of the "loose" liquid crystalline lattice, resulting in the formation of vesicles and tubules upon hydration. Hydration of **A-18U** (i.e., **A-18** with cis-unsaturation at the 9-positions) gave a large assortment of vesicles and tubules even at room temperature (Figure 2), as one would expect from a compound whose T_m undoubtedly lies far below room temperature.

Differential scanning calorimetry scans, obtained by heating 2 mg/mL gemini suspensions at 10° C/h in a calorimeter, gave endothermic peaks corresponding to T_m values of 33, 48, and 61 °C for **A-14**, **A-16**, and **A-18**, respectively (Figure 3). Only **A-l8** has a sharp peak indicative of cooperative melting in a tightly organized molecular array. When solid **A-14** and **A-16** were hydrated at 45 °C, optical microscopy images similar to those in Figure 2 were observed in contrast to the lack of bilayer formation at room temperature.

(31) Gaines, G. C. *Insoluble Monolayers at Liquid−Gas Interfaces*; Wiley: New York, 1966.
(32) Aston, M. S. *Chem. Soc. Rev.* **1993**, *22*, 67−71.
(33) (a) Menger, F. M.; Wood, M. G., Jr.; Richardson, S.; Zhou, Q.; Elrington, A. R.; Sherrod, M. J. *J. Am. Chem. Soc.* **1988**, *110*, 6797−6803. (b) Menger, F. M.; Richardson, S. D.; Wood, M. G., Jr.; Sherrod, M. J. *Langmuir* **1989**, *5*, 833−838.
(34) van Buuren, A. R.; Berendsen, H. J. C. *Langmuir* **1994**, *10*, 1703−1713.
(35) Matsumura, S.; Imai, K.; Yoshikawa, S.; Kawada, K.; Uchibori, T. *J. Am. Oil Chem. Soc.* **1990**, *67*, 996−1001.
(36) Fendler, J. H. *Membrane Mimetic Chemistry*; Wiley: New York, 1982.

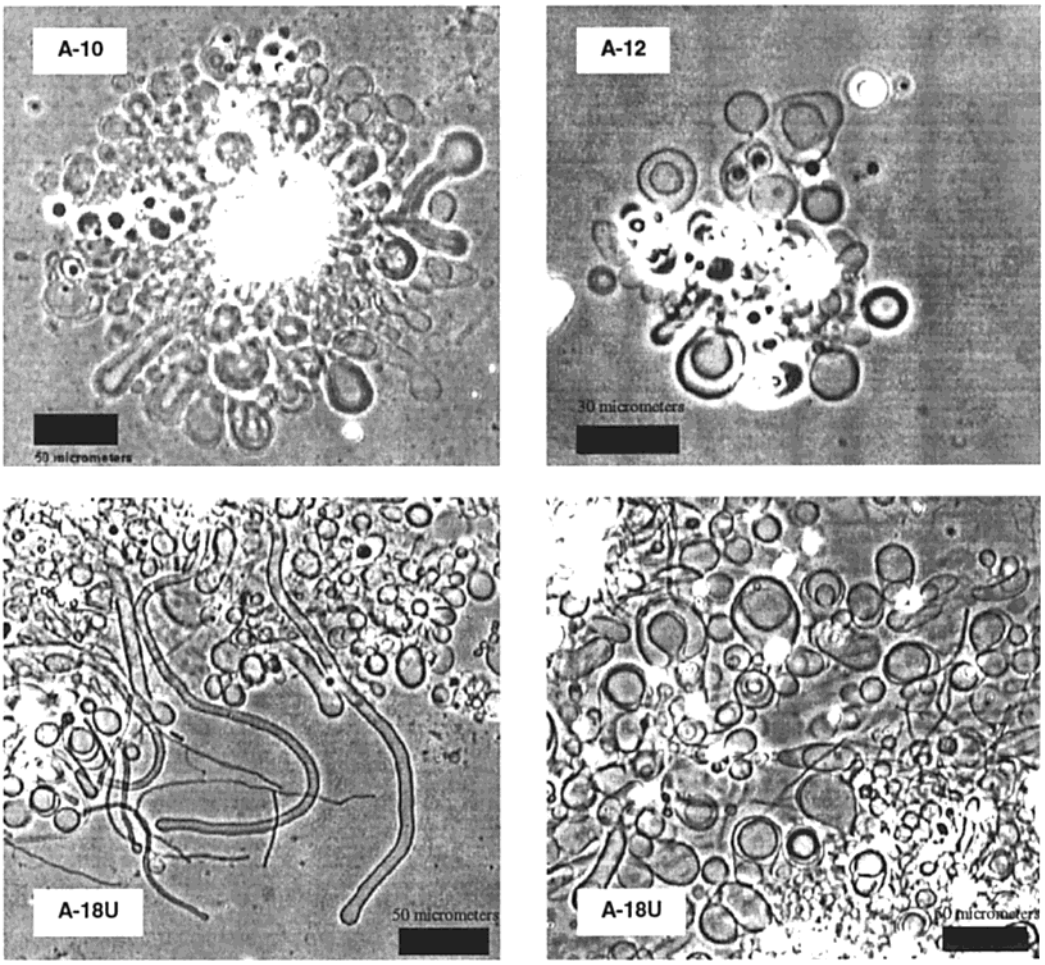

Figure 2. Phase contrast micrographs of vesicular and tubular structures of **A-10** (top left), **A-12** (top right), and **A-18U** (bottom) formed upon hydration for 3−4 h at 23 °C. Similar structures were observed for **A-14** and **A-16** samples incubated at 45 °C.

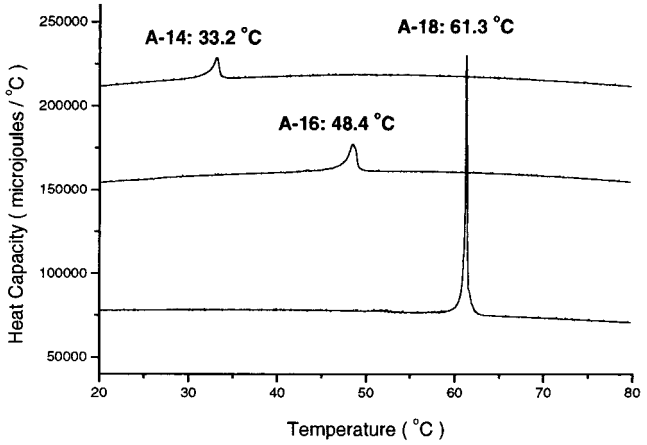

Figure 3. Endothermic peaks of 2 mg/mL suspensions of geminis **A-14**, **A-16** and **A-18**, obtained by differential scanning calorimetry (DSC) at a heating rate of 10 °C/h.

To summarize thus far: Series-A trehalose geminis, being water insoluble for chains of 10 or longer, form monomolecular films whose interfacial areas are dominated by the sugar spacers. Intermolecular chain/chain interactions stabilize the films. **A-8** forms small micelles in water, while upon hydration, higher homologues assemble into vesicular and tubular structures, visible by optical microscopy. The hydration properties are consistent with gel-to-liquid-crystal transitions, and, in fact, transition temperatures could be determined by calorimetry. Thus, the behavior of the trehalose geminis parallels that of phospholipids and synthetic double-chained surfactants.[17,37] It is as if the trehalose is less of a gemini spacer than a particularly large but conventional headgroup.

It will be noted that our gemini research draws upon many techniques including synthesis, film studies, light scattering, microscopy, calorimetry, and (as we shall soon see) tensiometry, conductimetry, and molecular mechanics. In colloid chemistry, a balanced perspective cannot be achieved by one methodology alone but only through the pursuit of consilience among multiple approaches.

Series-B Trehalose Geminis

We next pursued the idea of placing cationic groups on the trehalose derivatives in order to improve their water solubility. We experienced, it must be admitted, a degree of pleasure at the prospect of more manageable, water-soluble compounds. And thus did Series-B make its appearance. Immediately, however, new problems confronted us. Although **B-12** and **B-14** were obtained as pure compounds, this was not true for **B-16** and **B-18**. The latter two geminis, prepared in lower yields, gave satisfactory spectral data, but their elemental analyses deviated from theory by 1−2% (leading us to suspect the presence of an inorganic impurity). In any event, since **B-16** and **B-18** did not meet our criteria for high purity, we slighted them attentionwise in favor of their shorter cousins.

B-12 and **B-14** are indeed water-soluble compounds that form micelles above a critical micelle concentration (CMC), as

(37) Luisi, P. L.; Walde, P.; Eds. *Giant Vesicles*; Wiley: New York, 2000.

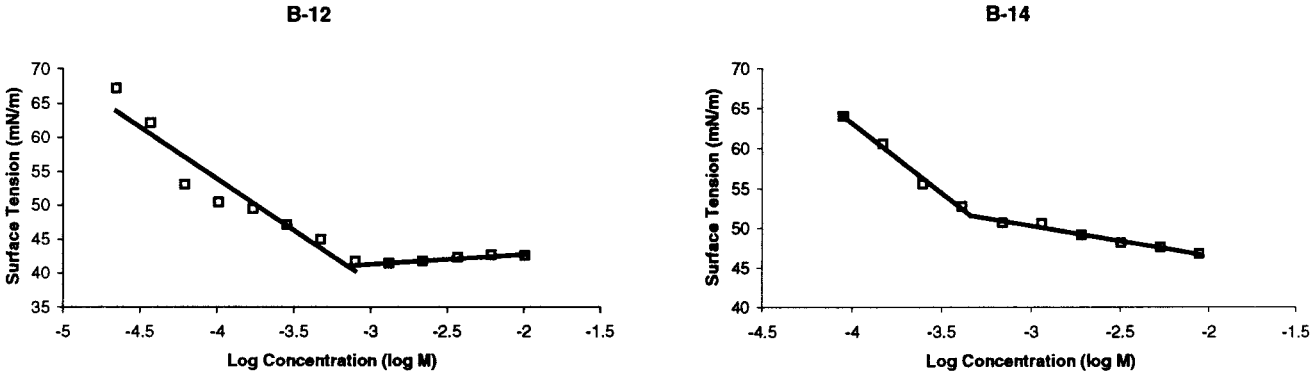

Figure 4. Tensiometry plots for the determination of **B-12** and **B-14** critical micelle concentrations at room temperature. **B-14** measurements were taken immediately after mixing, while **B-12** samples were aged for 20 min.

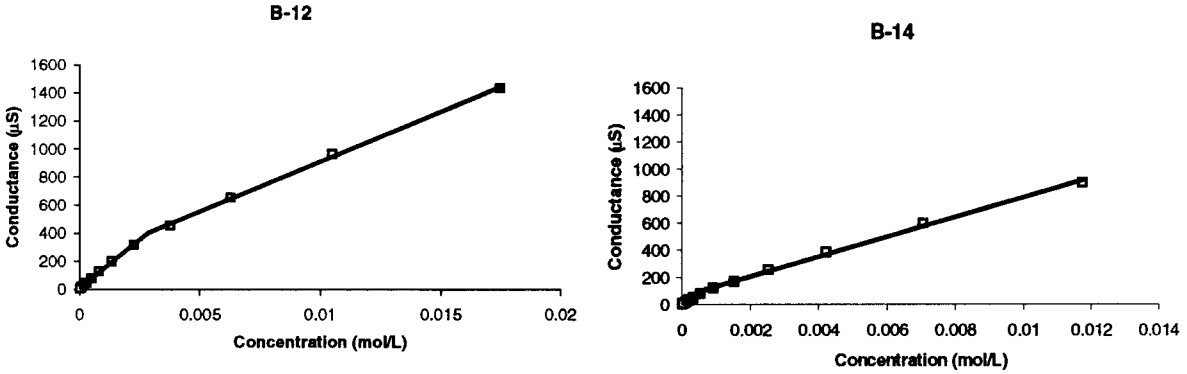

Figure 5. Plots giving **B-12** and **B-14** critical micelle concentrations as determined by breaks in the conductance vs concentration curve. Each point represents a single electrode reading at 23 °C.

Table 1

	CMC, mM[a]	
surfactant	surface tension conductance	surfactant
B-12	(0.7)	2.6
B-14	0.5	0.7
DTAC[b]	21	24
12-2-12[c]	1.0	

[a] Critical micelle concentration at 23 °C. [b] Dodecyltrimethylammonium chloride. [c] $C_{12}H_{25}N^+(CH_3)_2CH_2CH_2N^+(CH_3)_2C_{12}H_{25}$, 2 Br^-.[40]

indicated by dynamic light scattering which showed particles less than 5 nm in size. The CMC values were determined classically by the breaks in the surface tension versus concentration plots (Figure 4) and in the conductivity versus concentration plots (Figure 5).[38] The resulting data are given in Table 1 (along with data from two conventional surfactants for comparison purposes). As seen, the CMC values for **B-12** obtained tensiometrically and conductometrically (which are both reproducible) disagree badly. This discrepancy was traced, at least in part, to a time dependence of **B-12**'s surface tension. Thus, over the course of 10 min, the surface pressure of aqueous **B-12** solutions increased by as much as 10 mN/m after which it leveled off. Such dynamic surface tension processes, which have been observed previously with gemini surfactants,[13,15,39] are presumably related to difficulties that the geminis have, relative to conventional surfactants, in organizing at the air/water interface. To counter this problem, the **B-12** solutions in Figure 4 were aged for 20 min prior to the surface tension measurements, thereby lessening the possibility that the systems had not yet equilibrated. Despite this precaution, we cannot be certain that time-dependent interfacial reorganizations were not influencing the **B-12** plots and contributing to the disparity between the tensiometric and conductimetric-based data. The latter, of course, derive from a bulk property that is unaffected by interfacial events and are therefore more reliable. Interestingly, **B-14** shows no time-dependent surface tension, and the CMC values determined by the two methods are in reasonable agreement. Perhaps the longer chains enhance both the affinity for the air/water interface and the kinetics of interfacial absorption from solution.

Table 1 contains some salient comparisons. Judging from the conductimetric data, lengthening the chains from 12 to 14 carbons in the B-series diminishes the CMC about 4-fold (a sensitivity to chain length somewhat less than that found with conventional surfactants). **B-12** has a CMC an order of magnitude smaller than that of dodecyltrimethylammonium chloride (DTAC), a single-chained cationic surfactant. Once again, the enhanced propensity of geminis to self-assemble readily is affirmed.[1,39] Since **B-12** has only a 3-fold larger CMC than the sugarless gemini 12-2-12 (i.e., $C_{12}H_{25}N^+(Me)_2C_2H_4N^+(Me)_2C_{12}H_{25}$, $2Br^-$),[40] the sugar inhibits micellization to a relatively small degree, considering its multiple hydroxyls. Intermolecular hydrogen bonding at the micelle surface[41] seems to compensate for the enhanced hydrophilicity of the monomer.

Molecular Modeling

A central issue remains to be addressed: Why do Series-A geminis with 10 or more carbons form vesicles, while Series-B geminis prefer the micellar state? To properly confront this

(38) Rosen, M. J. *Surfactants and Interfacial Phenomena*; Wiley: New York, 1989.

(39) Rosen, M. J. *CHEMTECH* **1993**, *23*, 30−33.

(40) Menger, F. M.; Keiper, J. S.; Mbadugha, B. N. A.; Caran, K. L.; Romsted, L. S. *Langmuir* **2000**, *16*, 9095−9098.

(41) Venkatesan, P.; Cheng, Y.; Kahne, D. *J. Am. Chem. Soc.* **1994**, *116*, 6955−6956.

question, it was necessary to seek the assistance of molecular modeling. We could, thereby, assess whether the morphology has conformational roots.

Calculations began by inserting trehalose into the Macromodel program[42] and performing an AMBER* energy minimization on the structure. From a 25000-conformation search using the AMBER* force field, we selected the lowest-energy conformation which happened to be superimposable with the reported X-ray structure.[43,44] Next, the 6- and 6′-hydroxyls in this structure were replaced by an acetamido group. A 25000-conformation search was again carried out with AMBER* in a simulated water environment. The acetyl group was then replaced by a dodecanoyl, and yet another search was performed on the resulting **A-12** gemini. As it turned out, the overall conformation was dominated by two intramolecular hydrogen bonds between the amide carbonyls and the 2-hydroxyl groups of the neighboring glucose ring. The hydrogen bonds cause the two all-trans chains to swing away from each other by roughly 95°. This interaction was confirmed by the solid-state IR spectrum of **A-12**, which showed a carbonyl band at 1646 cm^{-1} as compared to 1700 cm^{-1} for Hecameg and a reported 1698 cm^{-1} band for the monomeric glucose analogues.[25] Reasoning that such a conformation would unrealistically preclude an intramolecular hydrophobic association, and that, in any event, solvent-swamping of the carbonyl hydrogen-bonding site was likely in water, we purposely disallowed the −C═O···HO− hydrogen bond and redid the calculations. In this manner we obtained Figure 6. It is seen that about eight carbons of one chain lie side-by-side with those of its partner chain. The N/N distance is only 7.4 Å, and the overall molecular shape is "tubular". Stated in another way, the sugar headgroup stretches over a distance not much larger than the width of the two chains as one would anticipate for a compound that is prone to pack into a bilayer.[45] Thus, as concluded earlier from experimental data, the trehalose acts more as a unifying headgroup than as a long spacer that can effectively isolate the chains.

The situation is quite different for Series-B geminis (Figure 7). The N/N distance is now 9.3 Å, causing the **B-12** molecule to have a conical rather than a tubular shape. It is believed that when the area of the headgroup exceeds the area of the chains, as it obviously does here, the formation of bilayers is disfavored, and micellization is the predominant mode of self-assembly.[45] Thus, micellization with Series-B is a direct result of conformational effects that create a more extended headgroup unit than with Series-A. Electrostatic repulsion among the cationic headgroups in Series-B may also play a role. Since micelles are less compact than bilayers, repulsive forces among the cationic headgroups of Series-B compounds favor micellization. Electrostatics cannot be the whole story, however, because double-chain cationics such as didodecyldimethylammonium bromide have no problems self-assembling into bilayers.[17]

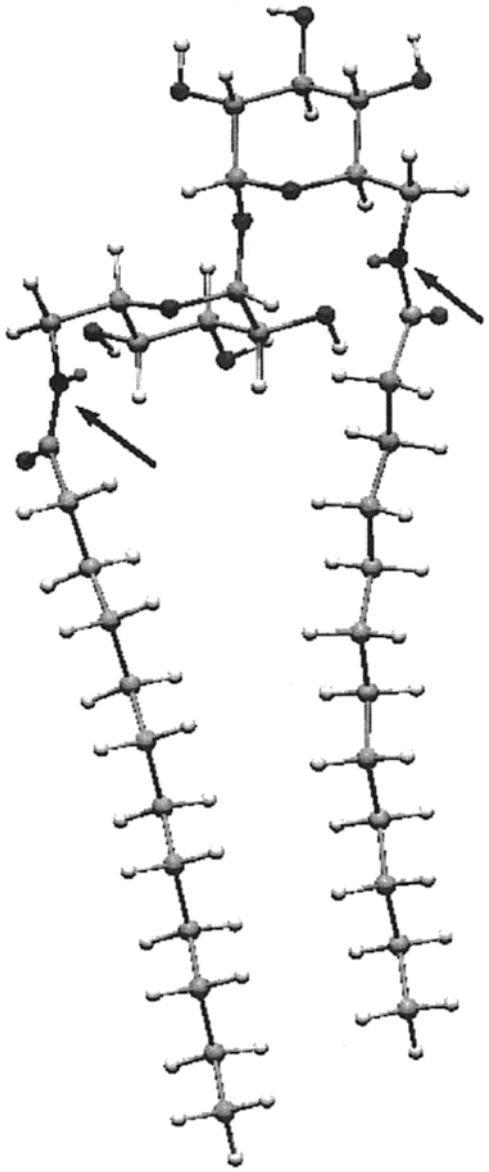

Figure 6. Macromodel snapshot of the lowest-energy conformation of **A-12** showing a tubular configuration characteristic of bilayer-forming amphiphiles. Arrows indicate amide nitrogens (N-to-N distance = 7.4 Å).

Conclusions

A series of gemini surfactants with a disaccharide (trehalose) spacer was synthesized such that the 6- and 6′-hydroxyls were substituted with long-chain amides (Series-A) or long-chain quaternary ammonium salts (Series-B). Different colloidal behavior was observed for the two series. Series-A geminis are water insoluble and form vesicular structures when hydrated or extruded in water. These structures were characterized by dynamic light scattering, microscopy, calorimetry, and molecular modeling. In addition, the compounds were deposited as monolayers on an aqueous subphase and examined with a surface balance. Series-B geminis, being water soluble, were subjected to tensiometry and conductimetry in addition to molecular modeling. Experimental data and theoretical analyses concur in defining the different morphologies assumed by the new surfactants. A correlation between morphology and structure was thereby uncovered.

Experimental Section

General Methods. All reagents were purchased from Aldrich. Solvents were dried over 4 Å molecular sieves. TLC was performed on Whatman normal phase silica plates and observed by UV or iodine visualization. Melting points were determined with a Thomas-Hoover capillary melting point apparatus and were uncorrected. ^{1}H NMR and ^{13}C NMR spectra were recorded on a Varian INOVA 300 or 400

(42) Mohamadi, F.; Richards, N. G. J.; Guida, W. C.; Liskamp. R.; Lipton, M.; Caufield, C.; Chang, G.; Hendrickson, T.; Still, W. C. *J. Comput. Chem.* **1990**, *11*, 440−467.

(43) Jeffrey, G. A.; Nanni, R. *Carbohydr. Res.* **1985**, *137*, 21−30.

(44) The Cambridge Structural Database: http://www.ccdc.cam.ac.uk/prods/csd.html.

(45) Israelachevilli J. *Intermolecular and Surface Forces*, 2nd ed.; Academic Press: London, 1991.

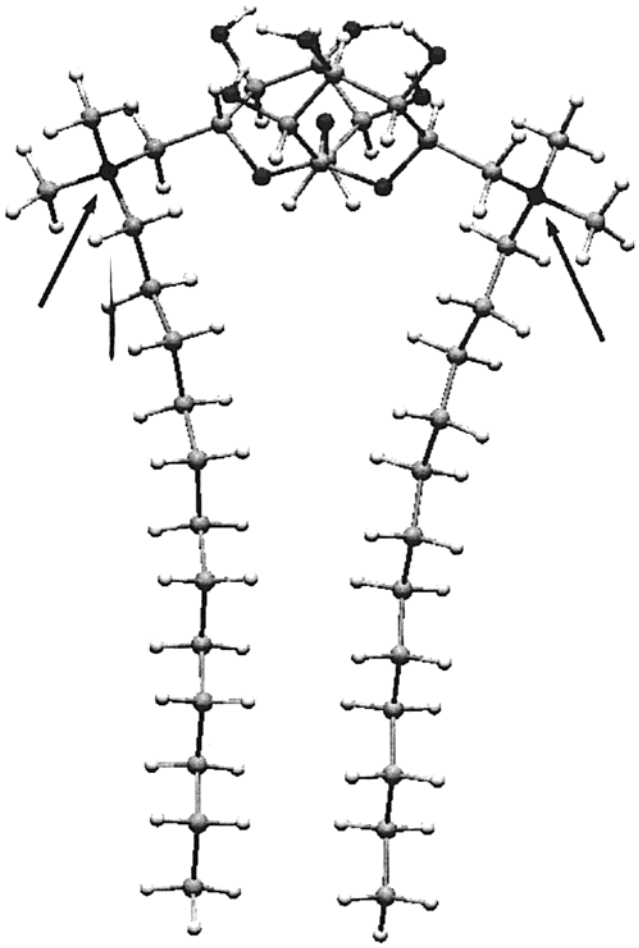

Figure 7. B-12 snapshot shows a "conical" conformation, as indicative of micelle-forming amphiphiles, with an N-to-N distance of 9.3 Å. Arrows indicate ammonium nitrogens.

spectrophotometer. Mass spectral data were obtained from the Emory University Mass Spectrometry Center; for this we acknowledge the use of Shared Instrumentation provided by grants from the NIH and the NSF. Elemental analyses were performed by Atlantic Microlab, Norcross, GA.

Hexa-*O*-acetyl-6,6′-di-*O*-toluene-*p*-sulfonyl-6,6′-dideoxy-α,α-D-trehalose 2.[28] Trehalose dihydrate (10.0 g, 26 mmol, 52 mmol equiv) was dissolved in 140 mL of pyridine. The solution color changed from lime green to pale yellow with the slow addition of 25.1 g (130 mmol) *p*-toluenesulfonyl chloride while stirring; heat was emitted. The reaction was complete in 35 min and the mixture quenched with 140 mL of acetic anhydride. After stirring overnight, the resulting dark solution was poured over approximately 1.5 L of ice water. The precipitate was collected and recrystallized from methanol three times to yield 3.2 g (14%) of **2** as a white solid, mp 162−164 °C; lit.[28] mp 170−172 °C.

^{1}H NMR (300 MHz, $CDCl_3$; C_2 denotes both C_2 and $C_{2'}$, etc.) δ 7.73 (d, J = 8.1, arom. H ortho to C−SO_2, 4H), 7.34 (d, J = 8.1 Hz, arom. H ortho to C−CH_3, 4H), 5.41 (t, J = 9.6 Hz, C_3, 2H), 4.92 (m, 6H), 4.10 (m, 6H), 2.44 (s, Me of Tos, 6H), 2.07 (s, C_2 Ac, 6H), 2.00 (s, C_3 Ac 6H), 1.98 (s, C_4 Ac, 6H).

^{13}C NMR ($CDCl_3$, 75 MHz) δ 170.09, 169.71, 145.48, 132.56, 130.04, 128.21, 92.96, 69.95, 69.34, 68.71, 68.31, 67.71, 21.83, 20.74.

FAB-HRMS (M + Li)$^+$: Calcd for 909.2133. Found: 909.2144.

Anal. Calcd for $C_{38}H_{46}O_{21}S_2$: C 50.55; H 5.14; S 7.10. Found: C 50.69; H 5.14; S 7.02.

2,3,4,2′,3′,4′-Hexa-*O*-acetyl-6,6′-diazido-6,6′-dideoxy-α,α-D-trehalose, 3.[28] To a solution of 14.9 g (16.5 mmol, 33 mmol equiv) ditosylated trehalose derivative **2** in 30 mL of 1,3-dimethyl-3,4,5,6-tetrahydro-2-(1H)-pyrimidinone (DMPU) was added 2.3 g (35.4 mmol) of NaN_3. The mixture was stirred in an oil bath at 90 °C for 6 h. The maroon-colored reaction mixture was quenched with water to produce a sticky orange precipitate. Two recrystallizations from methanol yielded 6.8 g of protected diazido trehalose **3** (64%), mp 115−117 °C; lit.[28] mp 114−116 °C.

^{1}H NMR ($CDCl_3$, 300 MHz): δ 5.47 (t, J = 9.9 Hz, C_3, 2H), 5.32 (d, J = 3.6 Hz, C_1, 2H), 5.12−4.96 (m, C_2 and C_4, 4H), 4.11−4.06 (m, C_5, 2H), 3.40−3.33 (m, C_6, 2H), 3.19−3.14 (m, C_6, 2H), 2.12 (s, C_2 Ac, 6H), 2.06 (s, C_3 Ac, 6H), 2.03 (s, C_4 Ac, 6H).

Anal. Calcd for: $C_{24}H_{32}N_6O_{15}$: C 44.72, H 5.00, N 13.04. Found: C 44.72, H 5.06, N 12.94.

General Procedure for the Staudinger Transformation of Diazide 3 to Diamides 4a−g. To a stirred solution of **3** and CH_2Cl_2, the appropriate acid chloride was injected by syringe. After stirring for 5 min, triphenylphosphine (PPh_3) dissolved in CH_2Cl_2 was added and the solution stirred for 2 days at room temperature. Bubbles were observed emerging from the reaction solution during the first few minutes (release of N_2). Reaction completion was revealed by normal-phase TLC (2:1 ethyl acetate:petroleum ether as eluent), which showed the formation of a very prominent UV−visible spot with R_f 0.3, corresponding to a triphenylphosphine salt byproduct. The mixture was washed with an aqueous $NaHCO_3$ solution (10 g/200 mL) and the organic solution dried over $MgSO_4$. The solvent was removed and purification was achieved via silica gel column chromatography (2:1 ethyl acetate:petroleum ether).

2,3,4,2′,3′,4′-Hexa-*O*-acetyl-6,6′-dioctanamido-6,6′-dideoxy-α,α-D-trehalose, 4a. According to the general procedure above, 2.1 g (3.3 mmol, 6.5 mmol equiv) of **3**, 50 mL of CH_2Cl_2 and 2.7 mL (9.8 mmol) of octanoyl chloride, and 2.4 g (9.2 mmol) of PPh_3 in 15 mL of CH_2Cl_2 were reacted. The dark solid was filtered, leaving a maroon-colored solution. After washing and drying, the resulting brown syrup was chromatographed to yield 2.2 g (80%) of **4a**, as a white solid, mp 70−72 °C.

^{1}H NMR (300 MHz, $CDCl_3$): δ 5.67 (t, J = 5.7 Hz, H on N, 2H), 5.46 (t, J = 9.9 Hz, C_3, 2H), 5.30 (d, J = 3.6 Hz, C_1, 2H), 4.93−4.84 (m, C_2 and C_4, 4H), 3.83 (m, C_5, 2H), 3.58−3. 52 (dd, J = 12.6, 6 Hz, C_6, 2H), 3.33−3.24 (m, C_6, 2H) 2.21−2.01 (m, α CH_2, 4H), 2.07 (s, C_3 Ac, 6H), 2.07 (s, C_4 Ac, 6H), 2.02 (s, C_2 Ac, 6 H), 1.62−1.60 (m, β CH_2, 4H), 1.28 (m, alkyl chain, 16H), 0.86 (t, J = 6.6 Hz, CH_3, 6H).

^{13}C NMR (75 MHz, $CDCl_3$): δ 173.25, 170.24, 169.93, 169.85, 91.87, 70.41, 69.87, 69.46, 69.23, 38.98, 36.86, 31.99, 29.57, 29.29, 25.77, 22.92, 21.00, 20.91, 14.41.

FAB-LRMS (M + Li)$^+$: 851.8

Anal. Calcd for $C_{40}H_{64}N_2O_{17}$: C 56.86, H 7.63, N 3.32. Found: C 56.81, H 7.71, N 3.15.

2,3,4,2′,3′,4′-Hexa-*O*-acetyl-6,6′-didecanamido-6,6′-dideoxy-α,α-D-trehalose, 4b. The reaction was carried out with 2.1 g (3.3 mmol, 6.5 mmol equiv) of **3**, 50 mL of CH_2Cl_2, 1.9 mL (9.0 mmol) of decanoyl chloride, and a solution of 2.2 g (8.4 mmol) of PPh_3 in 10 mL of CH_2Cl_2. Purification by silica gel column chromatography afforded 0.86 g (37%) of **4b**, mp 62−66 °C.

^{1}H NMR (400 MHz, $CDCl_3$): δ 5.68 (t, J = 6 Hz, H on N, 2H), 5.46 (t, J = 9.6 Hz, C_3, 2H), 5.30 (d, J = 3.6 Hz, C_1, 2H), 4.92−4.85 (m, C_2 and C_4, 4H), 3.85−3.81 (m, C_5, 2H), 3.57−3.52 (dd, J = 3.6, 10.8 Hz, C_6, 2H), 3.30−3.26 (m, C_6, 2H), 2.20−2.15 (m, α CH_2, 4H), 2.07 (s, C_3 Ac, 6H), 2.07 (s, C_4 Ac, 6H), 2.02 (s, C_2 Ac, 6H), 1.60 (m, β CH_2, 4H), 1.29−1.25 (m, alkyl chain, 24H), 0.87 (t, J = 6.8 Hz, CH_3, 6H).

^{13}C NMR (100 MHz, $CDCl_3$): δ 173.45, 170.43, 170.11, 170.04, 91.89, 70.39, 69.84, 69.44, 69.21, 38.90, 36.77, 32.06, 29.67, 29.54, 29.48, 25.67, 22.87, 20.88, 20.80, 14.32.

FAB-HRMS (M + Li)$^+$: Calcd for 907.4991. Found: 907.4974.

Anal. Calcd for $C_{48}H_{80}N_2O_{17}$: C 58.65, H 8.05, N 3.11. Found: C58.52, H 7.93, N 3.05.

2,3,4,2′,3′,4′-Hexa-*O*-acetyl-6,6′-didodecanamido-6,6′-dideoxy-α,α-D-trehalose, 4c. 3 (2.0 g, 3.2 mmol, 6.4 mmol equiv), 50 mL of CH_2Cl_2, 2.2 mL (9.8 mmol) of lauroyl chloride, and 2.20 g (8.4 mmol) of PPh_3 in 10 mL of CH_2Cl_2 were reacted. Silica gel chromatography of the orange-yellow syrup followed by recrystallization from hexane (to remove PPh_3 salt impurities detected by ^{1}H NMR) yielded 1.08 g (36%) of pure **4c**, mp 64−68 °C.

^{1}H NMR (400 MHz, $CDCl_3$): δ 5.64 (t, J = 6 Hz, H on N, 2H), 5.47 (t, J = 9.9 Hz, C_3, 2H), 5.31 (d, J = 3.9 Hz, C_1, 2H), 4.94−4.84 (m, C_2 and C_4, 4H), 3.83 (m, C_5, 2H), 3.58−3.52 (dd, J = 12.9, 6.3

Hz, C_6, 2H), 3.33−3.26 (m, C_6, 2H), 2.2−2.1 (m, α CH_2, 4H), 2.07 (s, C_3 Ac, 6H), 2.06 (s, C_4 Ac, 6H), 2.01 (s, C_2 Ac, 6H), 1.59 (m, β CH_2, 4H), 1.25 (m, alkyl chain, 32H), 0.88 (t, $J = 6.9$ Hz, CH_3, 6H).

^{13}C NMR (100 MHz, $CDCl_3$): δ 173.45, 170.42, 170.11, 170.03, 91.89, 70.38, 69.84, 69.43, 69.21, 38.90, 36.77, 32.11, 29.82, 29.71, 29.54, 25.67, 22.89, 20.88, 20.80, 14.33.

FAB-HRMS $(M + Li)^+$: Calcd for 964.5695. Found: 964.5668.

Anal. Calcd for $C_{48}H_{80}N_2O_{17}$ + 1/2 mol H_2O: C 59.67, H 8.45, N 2.90. Found: C 59.33, H 8.23, N 2.81.

2,3,4,2′,3′,4′-Hexa-*O*-acetyl-6,6′-ditetradecanamido-6,6′-dideoxy-α,α-D-trehalose, 4d. 3 (2.1 g, 3.2 mmol, 6.4 mmol equiv), 50 mL of CH_2Cl_2, 2.4 mL of myristoyl chloride (9.0 mmol), and 2.3 g of PPh_3 (8.8 mmol) in 10 mL of CH_2Cl_2 were reacted according to the general procedure. Purification by column chromatography of the light yellow syrup yielded 0.9 g (27%) **4d**, mp 56−60 °C.

^{1}H NMR (400 MHz, $CDCl_3$): δ 5.71 (t, $J = 6$ Hz, H on N, 2H), 5.46 (t, $J = 10$ Hz, C_3, 2H), 5.30 (d, $J = 4$ Hz, C_1, 2H), 4.92−4.84 (m, C_2 and C_4, 4H), 3.84−3.81 (m, C_5, 2H), 3.54−3.52 (m, C_6, 2H), 3.30−3.26 (m, C_6, 2H), 2.20−2.15 (m, α CH_2, 4H), 2.07 (s, C_3 Ac, 6H), 2.07 (s, C_4 Ac, 6H), 2.02 (s, C_2 Ac, 6H) 1.59 (m, β CH_2, 4H), 1.29−1.24 (m, alkyl chain, 40H), 0.87 (t, $J = 6.4$ Hz, CH_3, 6H).

^{13}C NMR (100 MHz, $CDCl_3$): δ 173.52, 170.43, 170.13, 170.06, 91.89, 70.38, 69.84, 69.42, 69.21, 38.89, 36.77, 32.12, 29.86, 29.73, 29.56, 25.68, 22.89, 20.88, 20.79, 14.33.

FAB-HRMS $(M + Li)^+$: Calcd for 1019.6243. Found: 1019.6274.

Anal. Calcd for $C_{52}H_{88}N_2O_{17}$: C 61.64, H 8.75, N 2.76. Found: C 61.69, H 8.86, N 2.64.

2,3,4,2′,3′,4′-Hexa-*O*-acetyl-6,6′-dihexadecanamido-6,6′-dideoxy-α,α-D-trehalose, 4e. The reaction was carried out with 2.1 g (3.2 mmol, 6.4 mmol equiv) of **3**, 50 mL of CH_2Cl_2, 2.7 mL (9.0 mmol) of palmitoyl chloride, and 2.4 g (9.1 mmol) of PPh_3 in 10 mL of CH_2Cl_2. Column chromatography of the off-white, sticky solid afforded 2.9 g (73%) of **4e** as a white crystalline solid, mp 54−57 °C.

^{1}H NMR (400 MHz, $CDCl_3$): 5.68 (t, $J = 6$ Hz, H on N, 2H), 5.46 (t, $J = 9.6$ Hz, C_3, 2H), 5.30 (d, $J = 3.6$ Hz, C_1, 2H), 4.92−4.85 (m, C_2 and C_4, 4H), 3.85−3.80 (m, C_5, 2H), 3.57−3.52 (m, C_6, 2H), 3.31−3.26 (m, C_6, 2H), 2.20−2.10 (m, α CH_2, 4H), 2.07 (s, C_3 Ac, 6H), 2.06 (s, C_4 Ac, 6H), 2.01 (s, C_2 Ac, 6H) 1.59 (m, β CH_2, 4H), 1.29−1.24 (m, alkyl chain, 48H), 0.87 (t, $J = 6.8$ Hz, CH_3, 6H).

^{13}C NMR (100 MHz, $CDCl_3$): δ 173.48, 170.43, 170.11, 170.04, 91.89, 70.38, 69.84, 69.42, 69.21, 38.90, 36.78, 32.12, 29.90, 29.73, 29.57, 25.68, 22.90, 20.88, 20.80, 14.33.

FAB-HRMS $(M + Li)^+$: Calcd for 1075.6869. Found: 1075.6865. $(M + H)^+$: Calcd for 1069.6787. Found: 1069.6749

Anal. Calcd for $C_{56}H_{92}N_2O_{17}$: C 62.90, H 9.05, N 2.62. Found: C 62.80, H 9.01, N 2.50.

2,3,4,2′,3′,4′-Hexa-*O*-acetyl-6,6′-dioctadecanamido-6,6′-dideoxy-α,α-D-trehalose, 4f. According to the general procedure, 2.2 g (3.4 mmol, 6.8 mmol equiv) of **3**, 50 mL of CH_2Cl_2, 1.9 mL (9.0 mmol) of stearoyl chloride, and 2.29 g (8.7 mmol) of PPh_3 in 10 mL of CH_2Cl_2 were reacted. **4f** (1.9 g, 50%), mp 53−56 °C, was isolated by silica gel chromatography of the sticky light orange solid.

^{1}H NMR (400 MHz, $CDCl_3$): δ 5.70 (t, $J = 6$ Hz, H on N, 2H), 5.45 (t, $J = 9.9$ Hz, C_3, 2H), 5.29 (d, $J = 3.6$ Hz, C_1, 2H), 4.92−4.86 (m, C_2 and C_4, 4H), 3.82 (m, C_5, 2H), 3.60−3.50 (m, C_6, 2H), 3.33−3.29 (m, C_6, 2H), 2.18−2.16 (m, α CH_2, 4H), 2.06 (s, C_3 Ac, 6H), 2.06 (s, C_4 Ac, 6H), 2.01 (s, C_2 Ac, 6H) 1.59 (m, β CH_2, 4H), 1.28−1.24 (m, alkyl chain, 56H), 0.86 (t, $J = 6.4$ Hz, CH_3, 6H).

^{13}C NMR (100 MHz, $CDCl_3$): 173.43, 170.41, 170.09, 170.02, 91.87, 70.37, 69.83, 69.42, 69.21, 38.89, 36.76, 32.12, 29.89, 29.73, 29.56, 25.67, 22.88, 20.87, 20.79, 14.33.

FAB-HRMS $(M + Li)^+$: Calcd for 1131.7495. Found: 1131.7443.

Anal. Calcd for $C_{60}H_{104}N_2O_{17}$ + 1 mol H_2O: C 63.02, H 9.34, N 2.45. Found: C 63.03, H 9.21, N 2.50.

2,3,4,2′,3′,4′-Hexa-*O*-acetyl-6,6′-di-(Z)-octadec-9-enamido-6,6′-dideoxy-α,α-D-trehalose, 4g. 3 (2.0 g, 3.1 mmol, 6.2 mmol equiv), 50 mL of CH_2Cl_2, 2.98 mL (9.0 mmol) of oleoyl chloride, and 2.2 g (0.4 mmol) of PPh_3 in 10 mL of CH_2Cl_2 were reacted. Purification by silica gel column chromatography afforded 0.8 g (23%) of **4g** as a hygroscopic, sticky solid, mp 50−56 °C.

^{1}H NMR (300 MHz, $CDCl_3$): 5.66 (t, $J = 5.6$ Hz, H on N, 2H), 5.48 (t, $J = 10$ Hz C_3, 2H), 5.36−5.34 (m, C═C, 4H), 5.32 (d, $J = 3.6$ Hz, C_1, 2H), 4.94−4.86 (m, C_2 and C_4, 4H), 3.86−3.82 (m, C_5, 2H), 3.58−3.54 (m, C_6, 2H), 3.33−3.26 (m, C_6, 2H), 2.22−2.20 (m, α CH_2, 4H), 2.09 (s, C_3 Ac, 6H), 2.08 (s, C_4 Ac, 6H), 2.03 (s, C_2 Ac, 6H), 2.01 (m, CH_2 α to C═C, 8H), 1.63 (m, β CH_2, 4H), 1.27 (m, alkyl chain, 40H), 0.89 (t, $J = 6.4$ Hz, CH_3, 6H).

FAB-HRMS $(M + Li)^+$: Calcd for 1127.7182. Found: 1127.7137.

Anal. Calcd for $C_{60}H_{100}N_2O_{17}$ + 1/2 mol H_2O: C 63.75, H 9.01, N 2.48. Found: C 63.55, H 8.93, N 2.44.

General Procedure for Deacetylation under Zémplen conditions.[25,46] The fully protected surfactants were stirred in a solution of 50 mL of MeOH and 2 mL of 0.57 M NaOMe/MeOH at room temperature overnight. Approximately 1.5 g of washed (acetone and methanol) Dowex MR-3 mixed bed ion-exchange resin was added, and the mixture stirred for 30 min, or until a pH of 7 was attained. The neutralized solutions were filtered, the solvent removed under reduced pressure, and the resulting solid dried in vacuo.

6,6′-Dioctanamido-6,6′-dideoxy-α,α-D-trehalose, A-8. 4a (1.5 g) was deacetylated as described above, to yield 1.0 g (95%) of **A-8**, mp 100−104 °C.

^{1}H NMR (300 MHZ, CD_3OD): δ 5.03 (d, $J = 3.3$ Hz, C_1, 2H), 3.85 (m, 2H), 3.74 (t, $J = 9.3$ Hz, 2H), 3.45 (m, 6H), 3.12 (t, $J = 9.3$ Hz, 2H), 2.20 (t, $J = 7.5$ Hz, α CH_2, 4H), 1.59 (m, β CH_2, 4H), 1.30 (m, alkyl chain, 16H), 0.88 (t, $J = 6.6$ Hz, CH_3, 6H).

^{13}C NMR (75 MHz, CD_3OD): δ 177.23, 95.68, 74.28, 73.48, 73.26, 72.22, 41.44, 37.18, 33.05, 30.51, 30.32, 27.29, 23.87, 14.60.

FAB-HRMS $(M + H)^+$: Calcd for 593.3661. Found: 593.3661.

Anal. Calcd for $C_{28}H_{52}N_2O_{11}$: C 56.74, H 8.84, N 4.73. Found: C 56.58, H 8.73, N 4.69.

6,6′-Didecanamido-6,6′-dideoxy-α,α-D-trehalose, A-10. 4b (0.8 g) was deacetylated to yield 0.6 g of (100%) **A-10** as a crystalline solid, mp 125−128 °C.

^{1}H NMR (400 MHZ, CD_3OD): δ 5.02 (d, $J = 4$ Hz, C_1, 2H), 3.86−3.83 (m, 2H), 3.73 (t, $J = 8.8$ Hz, 2H), 3.45−3.44 (m, 6H), 3.11 (t, $J = 8.8$ Hz, 2H), 2.20 (t, $J = 6.8$ Hz, α CH_2, 4H), 1.59 (m, β CH_2, 4H), 1.30 (m, alkyl chain, 24H), 0.88 (t, $J = 6.8$ Hz, CH_3, 6H).

^{13}C NMR (100 MHz, CD_3OD): δ 177.23, 95.69, 74.30, 73.49, 73.28, 72.23, 37.19, 33.22, 30.78, 30.66, 30.55, 27.30, 23.91, 14.62.

FAB-HRMS $(M + Li)^+$: Calcd for 655.4357. Found: 655.4350.

Anal. Calcd for $C_{32}H_{60}N_2O_{11}$ + 1/2 mol H_2O: C 58.43, H 9.35, N 4.26. Found: C 58.66, H 9.20, N 4.09.

6,6′-Didodecanamido-6,6′-dideoxy-α,α-D-trehalose, A-12. Deacetylation of **4c** under Zémplen conditions yielded 0.63 g (79%) of diamido trehalose derivative **A-12**, mp 168−172 °C.

^{1}H NMR (400 MHz, CD_3OD): δ 5.03 (d, $J = 3.3$ Hz, C_1, 2H), 3.86−3.84 (m, 2H), 3.74 (t, $J = 9.2$ Hz, 2H), 3.45−3.42 (m, 6H), 3.11 (t, $J = 10$ Hz, 2H), 2.19 (t, $J = 7.6$ Hz, α CH_2, 4H), 1.59 (m, β CH_2, 4H), 1.28 (m, alkyl chain, 32H), 0.88 (t, $J = 6.4$ Hz, CH_3, 6H).

^{13}C NMR (100 MHz, CD_3OD): δ 177.20, 95.66, 74.29, 73.48, 73.27, 72.21, 41.45, 37.18, 33.25, 30.96, 30.92, 30.81, 30.66, 30.56, 27.29, 23.91, 14.63.

FAB-HRMS $(M + Li)^+$: Calcd for 711.4983. Found: 711.4952.

Anal. Calcd for $C_{36}H_{68}N_2O_{11}$: C 61.34, H 9.72, N 3.97. Found: C 61.21, H 9.67, N 3.90.

6,6′-Ditetradecanamido-6,6′-dideoxy-α,α-D-trehalose, A-14. Deacetylation of 0.9 g of **4d** followed by drying in vacuo resulted in 0.6 g (88%) of **A-14**, mp 174−179 °C.

^{1}H NMR (400 MHz, CD_3OD): δ 5.05 (d, $J = 3.6$ Hz, C_1, 2H), 3.86−3.83 (m, 2H), 3.73 (t, $J = 9.2$ Hz, 2H), 3.45−3.41 (m, 6H), 3.11 (t, $J = 9.2$ Hz, 2H), 2.19 (t, $J = 7.2$ Hz, α CH_2, 4H), 1.58 (m, β CH_2, 4H), 1.27 (m, alkyl chain, 40H), 0.88 (t, $J = 6.8$ Hz, CH_3, 6H).

^{13}C NMR (100 MHz, CD_3OD): δ 177.22, 95.66, 74.30, 73.49, 73.29, 72.22, 41.46, 37.20, 33.26, 30.97, 30.83, 30.67, 30.57, 27.31, 23.92, 14.63.

FAB-HRMS $(M + Li)^+$: Calcd for 767.5609. Found: 767.5609.

Anal. Calcd for $C_{40}H_{72}N_2O_{11}$: C 63.13, H 10.07, N 3.68. Found: C 63.00, H 10.06, N 3.55.

6,6′-Dihexadecanamido-6,6′-dideoxy-α,α-D-trehalose, A-16. 4e (2.9 g) was deprotected under Zémplen conditions to afford 1.8 g (86%) of crystalline and hygroscopic **A-16**, mp 189−190 °C.

(46) Zémplen, G. *Ber. Dtsch. Chem. Ges.* **1927**, *60*, 1555.

^{1}H NMR (400 MHz, CD_3OD): δ 5.02 (d, J = 3.6 Hz, C_1, 2H), 3.85−3.83 (m, 2H), 3.74 (t, J = 9.2 Hz, 2H), 3.45−3.41 (m, 6H), 3.11 (t, J = 9.2 Hz, 2H), 2.19 (t, J = 7.6 Hz, 4H), 1.58 (m, β CH_2, 4H), 1.29−1.22 (m, alkyl chain, 48 H), 0.88 (t, J = 6.4 Hz, CH_3, 6H).

^{13}C NMR (100 MHz, CD_3OD): δ 177.18, 95.64, 74.30, 73.48, 73.28, 72.21, 41.45, 37.21, 33.26, 31.00, 30.84, 30.67, 30.57, 27.31, 23.92, 14.64.

FAB-HRMS $(M + Li)^+$: Calcd for 823.6235. Found: 823.6263.

Anal. Calcd for: $C_{44}H_{76}N_2O_{11}$ + 1/2 mol H_2O: C 63.97, H10.37, N 3.39. Found: C 64.13, H 10.32, N 3.30.

6,6′-Dioctadecanamido-6,6′-dideoxy-α,α-D-trehalose, A-18. While deacetylating 1.9 g of **4f** following the described protocol, the deprotected surfactant was observed precipitating from solution as a fine white solid. Vacuum-drying the collected white solid revealed 1.0 g (68%) of **A-18**, as a fine, white, hygroscopic solid, mp 192−196 °C.

^{1}H NMR: (400 MHz, 1:1 CD_3OD:$CDCl_3$, CHD_2OD peak used as reference): δ 5.17 (d, J = 4 Hz, C_1, 2H), 3.98 (m, 2H), 3.90 (t, J = 9.2 Hz, 2H), 3.70−3.61 (m, 4H), 3.53−3.48 (m, 2H), 3.29 (t, J = 9.2 Hz, 2H), 2.36 (t, J = 7.6 Hz, α CH_2, 4H), 1.77−1.73 (m, β CH_2, 4H), 1.45−1.41 (m, alkyl chain, 56H), 1.03 (t, J = 6.4, CH_3, 6H).

^{13}C NMR (100 MHz, 1:1 CD_3OD:$CDCl_3$, $CDCl_3$ peak used as reference): δ 176.74, 95.06, 73.51, 72.76, 72.45, 71.45, 40.96, 36.93, 32.66, 30.42, 30.27, 30.08, 26.69, 23.38, 14.49.

FAB-HRMS $(M + Li)^+$: Calcd for 879.6861. Found: 879.6832.

Anal. Calcd for $C_{48}H_{92}N_2O_{11}$ + 1/2 mol H_2O: C 65.35, H 10.62, N 3.18. Found: C 65.25, 10.40, 3.18.

6,6′-Di-(*Z*)-octadec-9-enamido-6,6′-dideoxy-α,α-D-trehalose, A-18U. Deacetylation of 0.8 g of **4g** yielded 0.6 g (100%) of **A-18U**, mp 154−158 °C.

^{1}H NMR (400 MHz, CD_3OD): δ 5.32 (t, J = 5.2 Hz, 4H), 5.02 (d, J = 4 Hz, 2H), 3.85−3.82 (m, 2H), 3.73 (t, J = 9.6 Hz, 2H), 3.45−3.41 (m, 6H), 3.29−3.28 (m, 2H), 3.11 (t, J = 10 Hz, 2H), 2.17 (t, J = 8 Hz, 4H), 2.02−2.00 (m, 8H), 1.58 (m, β CH_2, 4H), 1.31−1.27 (m, 40H), 0.88 (t, J = 6.4 Hz, CH_3, 6H).

^{13}C NMR (100 MHz, CD_3OD): δ 177.18, 131.04, 130.96, 95.68, 74.31, 73.49, 73.29, 72.22, 41.47, 37.19, 33.25, 31.02, 30.80, 30.64, 30.56, 30.43, 28.31, 27.31, 23.92, 14.64.

FAB-HRMS $(M + Li)^+$: Calcd for 875.6548. Found: 875.6555.

Anal. Calcd for $C_{48}H_{88}N_2O_{11}$ + 1/2 mol H_2O: C 65.65, H 10.21, N 3.19. Found: C 65.36, H 9.98, N 3.16.

6,6′-Diazido-6,6′-dideoxy-α,α-D-trehalose, 5.[28] Hexa-*O*-acetylated diazido trehalose **3** (2.8 g, 4.3 mmol), was deacetylated under Zémplen conditions to yield 1.6 g (94%) of deacetylated diazide **5**, mp 200−204 °C (with dec); lit.[28] mp 209−211 °C.

FAB-LRMS $(M + Li)^+$: 399.32; $(M + 2Li - H)^+$: 405.33; $(M + 3Li - 2H)^+$: 411.35.

6,6′-Diamino-6,6′-dideoxy-α,α-D-trehalose (di-HCl salt), 6.[47] Deacetylated diazide **5** (6.7 g, 17.0 mmol, 34 mmol equiv) was placed into a solution of 120 mL of dioxane and 24 mL of MeOH. PPh_3 (36.1 g, 137.8 mmol) was added, and the solution stirred under N_2 for an hour. NH_4OH (31 mL, 30% aqueous solution) was introduced and the mixture allowed to stir under N_2 overnight. The solvent was removed from the suspension of white solid by rotary evaporation. After drying in vacuo for 5 h, the solid was triturated with 150 mL of Milli Q water (18 MΩ·cm resistance) and the filtrate adjusted to pH 3 by careful addition of 0.1 M HCl. Residual PPh_3 and Ph_3PO were filtered and triturated with Milli-Q water. The aqueous filtrate was washed with toluene and then lyophilized to yield 6.5 g of a white solid that decomposed at 200 °C. Attempts to recrystallize from MeOH as the authors described[47] did not yield pure material in our hands. We found that some amount of the desired diamine salt was washing through with the MeOH filtrate. ^{1}H NMR showed only peaks for diamino trehalose dihydrochloride **6**. Thus, speculating that the impurities were inorganic salts, we opted to use the crude protonated diamine without further purification.

^{1}H NMR (400 MHz, CD_3OD): δ 5.3 (d, J = 3.6 Hz, C_1, 2H), 4.08 (t, J = 9.2 Hz, 2H), 3.90 (t, J = 9.2 Hz, 2H), 3.77−3.72 (m, J = 3.6, 2H), 3.51−3.41 (m, 4H), 3.38−3.20 (m, 2H).

(47) Fernández, J. M. G.; Mellet, C. O.; Blanco, J. L. J.; Mota, J. F.; Gadelle, A.; Coste-Sarguet, A.; Defaye, J. *Carbohydr. Res.* **1995**, *268*, 57−71.

FAB-HRMS $(M - HCl - Cl)^+$: Calcd for 341.1560. Found: 341.1573.

General Procedure for the Synthesis of Diammonium Trehalose Geminis B-12 and B-14. Molecular sieves (4 Å) were crushed, washed with MeOH, and then dried in a 110 °C oven overnight. To an oven-dried flask containing **6** and crushed molecular sieves, MeOH and the appropriate aldehyde were added. Pyridine−borane complex was injected into the flask by syringe, and the mixture stirred overnight under N_2. Reaction workup included stirring the solution for an hour with 10 mL of 6 N HCl, adjusting the pH to 14 with 1 M NaOH, and extracting the mixture with ether. After removing ether from the combined organic phases and drying in vacuo overnight, the resulting orange residue was triturated with MeOH to isolate any sieve particles. Rotary evaporation of MeOH left a glassy material that was quaternized with MeI in the presence of K_2CO_3 as base and MeOH as solvent. The mixture was stirred overnight, with a septum cover and a needle inserted for vent. The white solid isolated by drying the mixture was dissolved in Milli-Q purified water (18 MΩ·cm resistance) and extracted with $CHCl_3$. Rotary evaporation of solvent from the combined $CHCl_3$ phases was followed by crystallization from acetone. Filtration of the mixture yielded a white solid that was subsequently stirred in MeOH with Dowex (Cl^- form) ion-exchange resin overnight. Meanwhile, additional product was collected by passing the acetone filtrate through an ion-exchange column; the appropriate fractions were subjected to stirring with resin overnight to ensure complete ion exchange. After treatment with decolorizing charcoal, the resin-containing mixtures were filtered, dried, and then heated in acetone. The diammonium geminis were collected by filtration as white crystalline solids.

6,6′-*N*,*N*′-Didodecyldiamino-6,6′-dideoxy-α,α-D-trehalose, 7a. According to the general procedure above, 0.43 g of crushed 4 Å molecular sieves, 40 mL of MeOH, 2.25 mL (10.19 mmol) of dodecyl aldehyde, 2.04 g of crude diamine dihydrochloride **6**, and 0.80 mL (7.92 mmol) of pyridine−borane complex were reacted. After workup, 2.06 g of crude **7a** was isolated.

^{1}H NMR (CD_3OD, 400 MHz): δ 5.06 (d, J = 3.6 Hz, 2H), 3.89−3.88 (m, 2H), 3.52−3.46 (m, 2H), 3.10 (t, J = 9.6 Hz, 2H), 2.97−2.93 (m, 2H), 2.68−2.59 (m, 4H), 1.50 (t, J = 6.4 Hz, β CH_2, 4 H), 1.27 (m, 52H), 0.87 (t, J = 6.4 Hz, CH_3, 6H).

FAB-HRMS $(M + Li)^+$: Calcd for 683.5398. Found: 683.5377. $(M+H)^+$: Calcd for 677.5316. Found: 677.5300.

6,6′-*N*,*N*′-Tetramethyldidodecyldiammonium-6,6′-dideoxy-α,α-D-trehalose dichloride, B-12. The above product was quaternized with 0.91 g (6.58 mmol) of K_2CO_3 and 1.5 mL (24.1 mmol) of MeI followed by the ion-exchange and charcoal protocol described above, to yield 1.29 g (32% from crude diamine dihydrochloride **6**) of **B-12**, mp > 220 °C (with dec).

^{1}H NMR (400 MHz, CD_3OD): δ 5.11 (d, J = 3.9 Hz, 2H), 4.49−4.30 (m, 2H), 3.82−3.69 (m, 4H), 3.56−3.52 (m, 2H), 3.49−3.41 (m, 4H), 3.31 (m, α CH_2, 4H), 3.16−3.10 (m, 12 H), 1.79 (m, β CH_2, 4H), 1.37−1.30 (m, 36H), 0.90 (t, J = 6 Hz, CH_3, 6H).

^{13}C NMR (100 MHz, CD_3OD): δ 99.05, 74.74, 72.95, 72.69, 69.02, 68.82, 66.75, 66.49, 54.97, 52.67, 33.22, 30.91, 30.84, 30.75, 30.63, 30.50, 27.60, 23.88, 23.69, 14.61.

FAB-HRMS $(M - Cl)^+$: Calcd for 769.5709. Found: 769.5709.

Anal. Calcd for $C_{40}H_{82}Cl_2N_2O_9$: C 59.61, H 10.25, Cl 8.80, N 3.48. Found: C 59.35, H 10.31, Cl 8.83, N 3.51.

6,6′-*N*,*N*′-Tetramethylditetradecyldiammonium-6,6′-dideoxy-α,α-D-trehalose dichloride, B-14. Crude **6** (2.07 g), 0.44 g of crushed molecular sieves, 25 mL of MeOH, 2.48 g (11.68 mmol) of tetradecanal dissolved in 25 mL of $CHCl_3$, and 1 mL (9.9 mmol) of pyridine−borane complex were stirred at room temperature overnight and then at reflux for 30 min. After workup, 2.92 g of crude **7b**, was quaternized with 1.21 g (8.75 mmol) of K_2CO_3 and 2.1 mL (33.73 mmol) of MeI. 0.6 g (14% from crude **6**) of **B-14** was isolated as a white solid, mp > 200 °C (with dec) after the extractions, triturations, and ion-exchange procedures were performed as described above.

^{1}H NMR (400 MHz, CD_3OD): δ 5.07 (d, J = 3.6 Hz, 2H), 4.51 (t, poorly resolved, 2H), 3.86−3.72 (m, 4 H), 3.57−3.54 (m, 2H), 3.42 (m, 4H), 3.18 (16H) 1.80 (t, poorly resolved, β CH_2, 4H), 1.38−1.30 (m, 44H), 0.91 (t, J = 6.4 Hz, CH_3, 6H).

^{13}C NMR (100 MHz, CD_3OD) δ 98.94, 74.58, 72.89, 72.66, 68.80, 66.68, 66.47, 52.70, 33.20, 30.91, 30.84, 30.74, 30.61, 30.50, 27.58, 23.86, 23.69, 14.62.

FAB-HRMS $(M - Cl)^+$: Calcd for 825.6335. Found: 825.6310.

Anal. Calcd for $C_{44}H_{90}Cl_2N_2O_9$: C 61.30, H 10.52, Cl 8.22, N 3.25. Found: C 61.06, H 10.45, Cl 8.17, N 3.23.

CMC. (A) Surface tension measurements were made with a model 21 Fisher Surface Tensiomat apparatus according to the du Nuoy ring method. The 6 cm Pt/Ir ring was raised and lowered manually and was washed after analysis at each concentration, by dipping alternatively into 0.1 M HCl and Milli-Q purified water (18 MΩ·cm resistance), followed by flame-drying over a Bunsen burner. Solutions (25 mL) prepared with Milli-Q water in Pyrex crystallizing dishes were used. Reported values for **B-14** at each concentration are an average of 10 individual measurements, taken immediately after mixing. Due to the dynamic surface tension behavior of **B-12**, readings were taken at 20 min intervals (the ring was immersed in the solution during this aging period); the value reported is derived from the average of two measurements at each concentration. The time-dependent surface tension behavior was indicated by a constant increase over the 10 measurements at each concentration and later quantified by dynamic surface tension experiments conducted with the μTrough apparatus as described below.

(B) Conductivity experiments were performed with a YSI model 35 digital conductance meter at 23 °C. Solutions of each gemini in Milli-Q purified water were prepared in 25 mL glass culture tubes. Measurements were taken after several minutes when the reading stabilized, beginning with the lowest concentration solution, to avoid the need for washing the electrode between samples. When analysis of all solutions of a single surfactant was completed, the electrode was cleaned by rinsing with solvents in the order: acetone, methanol and Milli-Q water.

Differential Scanning Calorimetry (DSC). A Hart Scientific differential scanning calorimeter was used to measure the transition temperatures of the synthesized surfactants. Each of four metallic ampules or cells was cleaned by rinsing with solvents in the order: Milli-Q water, acetone, ethanol and methanol; caps were cleaned by rinsing with Milli-Q water and ethanol only, as the other solvents disturbed the rubber gaskets. Ampules and caps were dried in a 110 °C oven for at least 4 h and cooled to room temperature immediately before use. Mixtures containing 2 mg of surfactant/mL Milli-Q water were alternatively heated in a water bath and mixed by vortex (Scientific Products Deluxe Mixer) until an opaque suspension ensued. Mixtures were shaken before 500 μL aliquots were injected into the three sample cells using a Hamilton glass syringe; 500 μL of Milli-Q water was used as the standard in the calibration cell. The calorimeter was heated at a rate of 10 °C/h, with holding times of 30 and 10 min before scan-up and scan-down, respectively. Data were converted to heat capacity (μJ/°C) and plotted using Microcal Origin software. Three measurements were obtained for each surfactant to ensure the accuracy of the results. The 41.1 °C transition temperature observed for the standard, dipalmitoylphosphatidyl choline (DPPC), corresponded to the reported 41.2 °C value,[48] further validating the accuracy of our instrument.

Dynamic Light Scattering. A Coulter N4 Plus particle characterization instrument was used to determine the size of the surfactant aggregates. Cuvettes were rinsed with ethanol and Milli-Q water and dried with compressed air. Three-milliliter samples containing solutions prepared either at concentrations above the estimated or apparent CMCs (**A-8** and B-series respectively) or by diluting 500 μL extruded 1 mM vesicle solutions (**A-10**) were injected into the cuvettes using a syringe with an attached Whatman disposable filter (200 or 450 nm). Three individual measurements were taken at a scattering angle of 90° for each run, at 20 °C, with a prescale time of 2 min. A 2 min run time was used for **A-8** and **A-10**, while the B-series cationic surfactants were analyzed for 30 min. The statistical weight as opposed to intensity mode was selected, for a more accurate description of the population of a particular size of aggregate.

Film Balance. Pressure−area isotherm measurements were made with a Kibron μTrough located on a level marble table. The trough and Teflon barriers were thoroughly cleaned with ethanol and Milli-Q water and dried with compressed air before each measurement. The conducting pin was washed with ethanol and flame-dried over a Bunsen burner. Ten microliters of 1 mM stock solutions of each surfactant and a mixture of $CHCl_3$/MeOH (9/1 by volume) was carefully applied via a Hamilton glass syringe to the surface of a layer of Milli-Q water in the trough. After standing covered for 10 min to allow for evaporation of the solvents, the barriers were automatically compressed at a steady rate of 4 Å^2/chain/min and the obtained pressure/area data recorded by the instrument. After each run, the trough and accessories were vigorously cleaned, and the procedure was repeated 10 times for each surfactant. The μTrough apparatus was also used for quantifying the dynamic surface tension behavior displayed by **B-12** by inserting the conducting pin into freshly agitated solutions in Pyrex dishes; the change in surface pressure over time was thus monitored, and measurements were recorded by the instrument.

Preparation of Large Vesicles via Extrusion. The Avestin Liposofast extrusion apparatus was thoroughly cleaned with ethanol and Milli-Q water. An aqueous mixture of **A-10** (500 μL, 1 mM) was magnetically stirred for 3 h in a 5 mL round-bottom flask, yielding an opaque mixture, which was extruded 19 times through a 100 nm polycarbonate membrane.

Preparation of Giant Vesicles via Hydration.[17] Approximately 1 mg of surfactant was deposited within a 1.5 cm (inner diameter) rubber O-ring well, cemented to a borosilicate glass microscope slide. The sample was hydrated with 0.5 mL of Milli-Q water, a clean coverslip placed on top, and excess water wicked away, providing a tight seal. Trace sodium azide was added to the water to prevent bacterial contamination. **A-10**, **A-12**, and **A-18U** samples were allowed to stand at room temperature, while **A-14** and **A-16** samples were incubated at 45 °C using a Nikon Incubation warmer housed within a custom plastic incubation shell mounted on the Nikon Diaphot-TMD.

Molecular Modeling. Simulations were carried out with Macromodel[38] software on a Silicon Graphics computer. The available force fields were evaluated for the number of low-energy parameters in the energy minimizations of trehalose before AMBER*, which had no such parameters, was selected. For the 25 000 conformation searches performed, the ring carbons on the trehalose molecule were marked as chiral centers and water was chosen as the solvent. A comparison of all of the atoms in the working-set structure was conducted during the searches, and torsion bonds were selected. The structures used in the searches were the lowest-energy conformations from the preceding search. Thus, the lowest- energy conformation of the trehalose structure, from a 25 000 conformation search with AMBER*, was amended with an acetamido or a trimethyl ammonium group for the 6- and 6′-hydroxyls. The acetyl groups were then replaced by a dodecanoyl, and the trimethyl ammonium groups by a dimethyldodecyl ammonium moiety. Energy minimizations of these structures with AMBER* led to an all-*trans* orientation of the chains. The lowest-energy structures were subsequently subjected to yet another 25 000 conformation search with the torsion bonds deselected for all but the first methylene on each chain, followed by a search with the torsion bonds selected. For the **A-12** molecule, the C2- and C2′-hydroxyls were converted to methoxy groups to disallow for a hydrogen-bond interaction with the carbonyls of the amides on the neighboring glucose ring. Finally, an energy minimization was conducted on the lowest-energy conformation with the methoxy groups reverted back to hydroxyls, yielding the conformation shown in Figure 6. For the **B-12** diammonium gemini, conformation searches were performed for three structures, differing in the initial placement of the chains relative to the sugar moiety; the same lowest-energy conformation, shown in Figure 7, resulted in all three cases.

Acknowledgment. We thank Dr. Jim Snyder and Dr. Dennis Liotta for generously providing us with many hours' use of their Silicon Graphics workstation. We appreciate Dr. Jason Keiper's assistance with optical microscopy and Ben Cornett's helpful pointers with the Macromodel modeling. This work was supported by the Army Research Office.

JA0033178

(48) Racansky, V.; Valachovic, D.; Balgavy, P. *Acta Phys. Slovaca* **1987**, *37*, 166−176.